Published in final edited form as:
J Nutr Biochem. ; : 108441. doi:10.1016/j.jnutbio.2020.108441.

Development of insulin resistance preceded major changes in iron homeostasis in mice fed a high-fat diet☆

Joe Varghese[a,1,**], **Jithu V James**[a,1], **R Anand**[a], **Muthuraman Narayanasamy**[a], **Grace Rebekah**[b], **Banumathi Ramakrishna**[c,2], **Arun Jose Nellickal**[d], **Molly Jacob**[a,*]

[a]Department of Biochemistry, Christian Medical College, Vellore 632002, Tamil Nadu, India

[b]Department of Biostatistics, Christian Medical College, Vellore 632002, Tamil Nadu, India

[c]Department of Pathology, Christian Medical College, Vellore 632002, Tamil Nadu, India

[d]Department of Clinical Biochemistry, Christian Medical College, Vellore 632002, Tamil Nadu, India[3]

Abstract

Type 2 diabetes mellitus (T2DM) and insulin resistance (IR) have been associated with dysregulation of iron metabolism. The basis for this association is not completely understood. To attempt to investigate this, we studied temporal associations between onset of insulin resistance (IR) and dysregulated iron homeostasis, in a mouse model of T2DM.

Male C57Bl/6 mice (aged 8 weeks) were fed a high-fat diet (HFD; 60% energy from fat) or a control diet (CD; 10% energy from fat) for 4, 8, 12, 16, 20 and 24 weeks. Development of IR was documented, and various metabolic, inflammatory and iron-related parameters were studied in these mice.

HFD-feeding induced weight gain, hepato-steatosis and IR in the mice. Onset of IR occurred from 12 weeks onwards. Hepatic iron stores progressively declined from 16 weeks onwards. Accompanying changes included a decrease in hepatic hepcidin (*Hamp1*) mRNA expression and serum hepcidin levels and an increase in iron content in the epididymal white adipose tissue (eWAT). Iron content in the liver negatively correlated with that in the eWAT. Factors known to regulate hepatic *Hamp1* expression (such as serum iron levels, systemic inflammation, and bone marrow-derived erythroid regulators) were not affected by HFD-feeding. In conclusion, the results show that the onset of IR in HFD-fed mice preceded dysregulation of iron homeostasis, evidence of which were found both in the liver and visceral adipose tissue.

[*]Correspondence to: Department of Biochemistry, Christian Medical College, Bagayam, Vellore – 632002, India. Tel.: +91 416 2284267. joevarghese@cmcvellore.ac.in (J. Varghese), mjacob@cmcvellore.ac.in (M. Jacob).
[3]Affiliated to The Tamil Nadu Dr. MGR Medical University, Chennai, India.
[1]Co-first authors.
[2]Current affiliation: Department of Histopathology, SRM Institutes for Medical Science, Vadapalani, Chennai, India.

Declaration of competing interest
The authors have no conflicts of interest to declare.

Author contributions
JV and JVJ carried out the experimental work. AJN, MN and AR carried out some of the assays. BR carried out the histopathological analysis and interpreted the data. GR helped with statistical analysis of the data. JV and MJ designed the study, analyzed and interpreted the data and wrote the manuscript. All authors read and approved the final version of the manuscript.

Keywords

Insulin resistance; Hepcidin; High-fat diet; Iron; Hepatic iron content; Adipose tissue iron

1 Introduction

Insulin resistance (IR) is the hallmark of type 2 diabetes mellitus (T2DM). It is characterized by impaired sensitivity of tissues to the actions of insulin [1]. Several studies have shown a strong association between high levels of serum ferritin (a marker of body iron stores) and increased risk of T2DM [2–6]. However, ferritin is an acute phase reactant; its levels in blood are also increased in response to inflammation [7,8]. Since T2DM is associated with chronic low-grade inflammation [9], it is possible that the raised serum ferritin levels seen in T2DM may be secondary to this, rather than to increased iron stores *per se*. Such a possibility is supported by the results of the recent EPIC-InterAct study, which showed that though serum ferritin was associated with increased risk of T2DM, other markers of iron status (such as transferrin saturation and serum iron) were not [10]. However, there are also reports that the association between serum ferritin and IR remained significant, even after adjusting for inflammation [11]. Improvements in insulin sensitivity have been shown to occur following depletion of iron stores (by phlebotomy), both in patients with T2DM and in healthy individuals [12,13]. These studies seem to suggest that increased body iron *per se*, and not inflammation, may mediate the link between increased serum ferritin levels and T2DM. These variable observations indicate that the mechanisms that underlie such associations are complex and not completely understood.

Hepcidin, a peptide synthesized and secreted mainly by the liver, is the chief regulator of systemic iron homeostasis [14]. A number of factors regulate hepatic hepcidin (*Hamp1*) expression; these include liver iron stores, serum iron levels, inflammation and the erythropoietic drive [15]. Regulation of *Hamp1* expression in response to changes in liver and serum iron levels is mediated predominantly through signaling via the BMP-SMAD pathway [16]. BMP6 (secreted by hepatic sinusoidal cells [17]) up-regulates hepatic *Hamp1* expression [18], while matriptase-2, a membrane-associated serine protease, has the opposite effect [19,20]. Hepatic iron stores have been shown to regulate BMP6 [21] and matriptase-2 [22,23].

Hepcidin is known to be robustly down-regulated by factors secreted by the bone marrow, in response to increased erythropoietic activity [24]. Although the identities of these factors (collectively known as ‘erythroid regulators’ of hepcidin) are not clearly known, erythroferrone (ERFE), growth differentiation factor-15 (GDF-15) and twisted gastrulation factor 1 (TWSG1) have been proposed to be candidate molecules [24]. Insulin has been shown to stimulate erythropoiesis *in vitro* [25,26]. However, the effect of hyperinsulinemia, which is a characteristic feature of IR [27], on the expression of the erythroid regulators (and consequently on hepcidin) *in vivo* is not known. Systemic inflammation has been shown to induce *Hamp1* via interleukin-6 (IL-6) [28]. Whether IR-associated inflammation [9,29] has a significant effect on hepcidin is not known.

High-fat feeding in mice is known to be associated with IR and dysregulation of iron homeostasis [30–32]. However, the temporal association between onset of these 2 conditions, under these circumstances, is not clear. For example, it is not known whether iron dysregulation precedes or follows IR in this setting. Such knowledge would provide insights into interactions that occur in the pathogenesis of these 2 conditions, both of which are of considerable clinical relevance. In addition, the effect of IR on hepcidin and the various factors that regulate it (as described above) is not known. Such information would also provide insights into the processes involved in the development of these conditions. In an attempt to answer these questions, we carried out a time-course study in C57Bl/6 mice fed a high-fat diet, which is a commonly used mouse model of T2DM [33].

2 Methods

2.1 Animals

All experiments were carried out with the approval of the Institutional Animal Ethics Committee at Christian Medical College, Vellore, India (IAEC No. 14/2013), in accordance with the regulations of the Committee for the Purpose of Control and Supervision of Experiments on Animals (CPCSEA), Government of India.

At 7 weeks of age, male C57BL/6J mice were shifted from a “chow” diet (Diet no. #D131, Scientific Animal Food and Engineering, France) to a control diet (CD) (Research Diets, Inc., USA, #D12450J, with 10% of total energy derived from fat). At 8 weeks of age, mice were randomly allocated to receive either a high-fat diet (HFD) (Research Diets, USA, #D12492, with 60% of total energy derived from fat) or continued on CD for 4, 8, 12, 16, 20 or 24 weeks. The iron content of the chow diet used was 250 mg/kg and that of CD and HFD were 43 mg/ kg and 58 mg/kg respectively [30,34,35]. Weight gain in each mouse was monitored at weekly intervals. A subset of HFD-fed and CD-fed mice (n=6 in each group) were euthanized by cervical dislocation under deep inhalational anesthesia (using isoflurane) at the end of each of the time points studied. At the time of euthanasia, blood was collected from the inferior vena cava. The liver and epididymal white adipose tissue (eWAT) (representative of visceral adipose tissue in rodents [36]) were isolated, and each was weighed. These were snap-frozen in liquid nitrogen and stored at −70 °C till further analysis. The tibia and femur from both hind limbs were removed and used for isolation of bone marrow.

All mice were housed in static cages in a conventional animal facility, were exposed to standard 12-h light/dark cycle and had access to food and water *ad libitum*. All the cages contained environment enrichment in the form of plastic or cardboard tunnels. We have used the ARRIVE checklist when writing our report [37].

2.2 Evaluation of insulin sensitivity in vivo

Intraperitoneal glucose tolerance tests (ipGTT) and insulin tolerance tests (ITT) were carried out to determine glucose tolerance and insulin sensitivity, as described earlier [38,39]. These were done at baseline and towards the end of the periods of feeding, 3 and 2 days prior to euthanasia, respectively.

2.3 Isolation of erythroid progenitor cells (Ter119$^+$ cells) from bone marrow

Single-cell suspensions of bone marrow were prepared as described previously [40]. These were used for isolation of Ter119$^+$ cells (erythroid precursors), by magnetically activated cell sorting (Octo-MACS) using anti-mouse Ter119 MicroBeads, according to the manufacturer's instructions (Miltenyi Biotec, Germany).

2.4 Quantitative real-time PCR (qPCR)

RNA was isolated from the liver, adipose tissue and Ter119$^+$ cells (isolated from bone marrow), using Tri-Reagent (Sigma, India), according to the manufacturer's instructions. RNA isolates were subjected to DNase I treatment (Ambion DNA-free kit). RNA integrity was confirmed by denaturing agarose gel electrophoresis. One microgram of RNA was used to synthesize cDNA, using the Reverse Transcriptase Core Kit (Eurogentec, Belgium). Quantitative PCR reactions were carried out in duplicates, using the Takyon qPCR SYBR master mix (Eurogentec, Belgium) and a BioRad Chromo4 real-time PCR machine. The expression levels of genes of interest were normalized to *Rpl19*, which was used as the reference gene. Sequences of all primers used, and primer validation data are shown in Supplementary Table 1.

2.5 Western blotting

Western blotting was carried out as described previously [41]. Briefly, snap-frozen liver and adipose tissue samples were homogenized in ice-cold RIPA buffer. Processed samples, containing 50 μg protein, were heat-denatured in Laemmli buffer and separated on 10% SDS-PAGE gels. Separated proteins were electro-transferred onto PVDF membrane (0.45 μm, Immobilon-P, Millipore, Merck, Germany) at 80 V for 2 h. After completion of the transfer, the membranes were blocked with 5% BSA (in TBS-T), at room temperature for 2 h, and later probed with the specific primary antibodies, with incubations carried out overnight at 4 °C. This was followed by incubation with appropriate secondary antibody (2 h at room temperature). Bands were detected using a chemiluminescence substrate kit (SuperSignal West Dura, Thermo Fisher Scientific, USA), using a gel documentation system (Fluorochem SP, Alpha Innotech, USA). The intensities of the bands were quantified using ImageJ software (NIH, USA), and normalized to that of β-actin, which was used as a loading control. Sources and dilutions of primary and secondary antibodies used are given in Supplementary Table 2.

2.6 Tissue iron estimation

For liver iron estimation, acid extracts were prepared and iron content was estimated by a colorimetric assay based on bathophenanthrolene-dye binding as described earlier [41]. Atomic absorption spectrophotometry (AAS) was used to estimate iron content in adipose tissue samples. Approximately 100 mg of eWAT was weighed and homogenized in 500 μL of RIPA buffer. The homogenate was centrifuged at 14,000×*g* for 10 min; the fat that accumulated at the top was removed and the centrifugation step was repeated. The supernatant obtained (100 μL of it) was digested by adding acid reagent (3 M hydrochloric acid and 10% TCA) (1:2 v/v) and incubating at room temperature for 30 min. It was then centrifuged at 12,000×*g* for 10 min. The supernatant obtained was used for estimation of

iron, using a Perkin-Elmer AA200 atomic absorption spectrometer. A Perkin-Elmer iron hollow cathode lamp was used as the light source and an atomization temperature of 2300 °C was provided by an air-acetylene flame. Slit width of 0.2 nm and wavelength of 248.3 nm were used as spectrometer parameters. The iron content in each sample was calculated based on readings obtained from a set of working standards prepared by serial dilution of a stock standard solution of iron (1000 μg/mL, cat. no. 02583, Sigma, India). Results were normalized to the wet weight of tissue processed.

2.7 Visualization of tissue iron by Perls' perfusion staining

In situ Perls' Prussian blue perfusion staining was done as described previously [32]. Briefly, mice under terminal anesthesia, were perfused (via cardiac puncture) with 30 mL of phosphate-buffered saline containing heparin (5 U/mL), at a rate of 6 mL/min. Following this, perfusion was continued at the same rate with 75 mL of a solution containing 4% paraformaldehyde, 1% potassium ferrocyanide, and 1% HCl (Prussian blue staining solution). One hour after the end of perfusion, the liver was removed from the animal for gross examination; photographs were taken of the organ.

2.8 Liver triglyceride estimation

Liver triglyceride levels were estimated, as previously described [42]. Lipids from liver tissue were extracted in chloroform/methanol/water (8:4:3 [v/v/v]), by Folch's extraction procedure. The triglyceride content of the extracted lipid was estimated, using a commercially available kit (#TR212, Randox, UK).

2.9 Biochemical analyses of serum samples

Serum samples were used for estimation of the following analytes, using commercially available ELISA kits: insulin (#10–1247-01, Mercodia, Sweden), hepcidin (#S-1465.0001, Peninsula Laboratories, USA), ferritin (#Ab157713, Abcam, UK), adiponectin (#MRP300, R&D Systems, USA), erythropoietin (#MEP00B, R&D Systems, USA), C-reactive protein (#MCRP00, R&D Systems, USA), GDF-15 (#DT6385, R&D Systems, USA) and interleukin-6 (#DY406–05, R&D Systems, USA). All assays were carried out as per manufacturers' instructions. Serum levels of iron were estimated, using a colorimetric assay based on bathophenanthrolene dye-binding as described earlier [41]. Serum triglyceride was estimated using a commercially available kit (#10010303, Cayman Chemicals, USA).

2.10 Histological examination of liver

Liver tissue was fixed in 10% buffered formalin, embedded in paraffin and four-micron thick sections were made for histological examination. Tissue sections were stained with hematoxylin and eosin (H&E) for light microscopy. Additional sections were stained with Prussian blue for visualization of iron deposits in the liver (Perls's staining). All slides were examined by a trained histopathologist. Grading of steatosis was done based on standard criteria [43]. Accordingly, steatosis was graded as mild (<33%), moderate (33–66%) or severe (> 66%) depending upon the proportion of hepatocytes that showed steatotic changes. Photographs were obtained using an Olympus DP21 digital camera attached to an Olympus BX43 light microscope.

Europe PMC Funders Author Manuscripts

2.11 Statistical analysis

Statistical Package for Social Scientists (SPSS), version 16.0, was used for all statistical analyses. Two-way analysis of variance (two-way ANOVA) was used; *P* values for effects of the type of diet and duration of feeding, and interactions between the 2 were reported. Post-hoc pair-wise comparisons were made, using the Bonferroni test. In all cases, $P<0.05$ was used to indicate statistical significance. Correlation analyses were done by Spearman's correlation test. All variables with a *P* value <0.1 on univariate analyses were included in multivariate linear regression analyses models.

3 Results

3.1 High-fat feeding increased body weight and induced hepatosteatosis, glucose intolerance, insulin resistance and hyperinsulinemia in mice

Over the period of the study, HFD-fed mice progressively gained weight, while body weights in CD-fed mice were not significantly affected. The weight gains in HFD-fed mice were significantly higher than those seen in CD-fed mice from 8 weeks onwards (Fig. 1A). Weights of eWAT in HFD-fed mice increased progressively up to 16 weeks, after which it tended to decline. CD-fed mice did not show significant changes in eWAT weights over the period of the study (Fig. 1B). Liver weights in HFD-fed mice were significantly higher than those from CD-fed mice, from 20 weeks onwards. Liver weights in CD-fed mice were similar at all the time points studied (Fig. 1C). The content of triglycerides in the liver increased progressively, with increasing duration of feeding in mice fed HFD; this was not seen in those fed CD. HFD-fed mice showed significantly higher triglyceride content compared to CD-fed mice, from 12 weeks onwards (Fig. 1D). This was associated with histologically visible steatosis, which was mild at 12 weeks, moderate at 16 and 20 weeks, and severe at 24 weeks (Supplementary Fig. 1).

HFD-feeding induced glucose intolerance in the mice (as assessed by ipGTT), from as early as 4 weeks after initiation of feeding. However, there was no significant worsening of glucose tolerance with continuing HFD-feeding for up to 24 weeks (Fig. 1E and Supplementary Fig. 2A). Results of the ITT in HFD-fed mice showed a progressive increase in IR, which was significantly greater than that in CD-fed mice, from 12 weeks onwards (Fig. 1F and Supplementary Fig. 2B). CD-fed mice did not show significant changes in glucose tolerance (Fig. 1E) or IR (Fig. 1F) at the time points studied. Serum insulin levels increased progressively with duration of feeding in HFD-fed mice, but not in those fed CD. Levels were significantly higher in HFD-fed mice than in CD-fed mice, at 20 and 24 weeks (Fig. 1G). Serum adiponectin levels increased initially in response to HFD (up to 12 weeks) but declined at later time points. Levels were significantly higher in HFD-fed mice than in CD-fed mice, at 8, 12, and 16 weeks. No significant changes were seen in CD-fed mice (Fig. 1H). Serum triglyceride levels were not affected by CD or HFD at any of the time points studied (Supplementary Fig. 2C).

3.2 HFD-feeding decreased hepatic hepcidin expression and serum hepcidin levels

Both the type of diet and duration of feeding were found to individually affect hepatic *Hamp1* expression (Fig. 2A) and serum hepcidin levels (Fig. 2B); however, no significant

Europe PMC Funders Author Manuscripts

interaction was found between the two. Overall, HFD-fed mice had lower hepatic *Hamp1* expression and serum hepcidin levels than CD-fed mice (Fig. 2A and B). *Hamp1* mRNA expression in the liver and serum hepcidin levels correlated positively with each other (Fig. 2C).

3.3 HFD-feeding decreased hepatic iron content and caused changes in expression of iron-related proteins in the liver

In mice fed CD, there was a progressive increase in hepatic iron content with increasing duration of feeding; these increases were significant at 20 and 24 weeks compared to baseline (0 weeks). Mice fed HFD, however, had significantly lower hepatic iron content compared to those fed CD, from 16 weeks onwards (Fig. 3A). This was associated with significant decreases in protein levels of ferritin, the iron storage protein (at 20 and 24 weeks) (Fig. 3B). In situ Perls' Prussian blue perfusion staining for iron showed decreased staining of the liver in mice fed HFD for 24 weeks (Fig. 3D), confirming reduced iron content in the organ. Perls' staining for iron in tissue sections of liver obtained from CD and HFD-fed mice did not show stainable iron (data not shown).

Both the type of diet and duration of feeding had individual significant effects on *Tfrc* mRNA expression, with levels tending to be higher in HFD-fed mice (Fig. 3C). HFD-feeding did not significantly affect gene expression and protein levels of ferroportin (Fig. 3E and F). However, there was a negative correlation between *Tfrc* mRNA levels and ferroportin protein levels in the liver (Spearman's correlation coefficient=−0.278, P=0.018). Expression of mRNA for BMP6 and matriptase-2, and mRNA and protein levels of TfR2 in the liver were not affected by HFD-feeding (data not shown).

3.4 HFD-feeding did not affect serum iron levels, markers of inflammation or proteins involved in duodenal iron absorption

HFD-feeding did not significantly affect serum levels of iron at any of the time points studied (Fig. 4A). Serum ferritin levels increased with increasing durations of feeding and tended to be higher in HFD-fed mice; however, this effect was not statistically significant (diet effect P=0.156) (Fig. 4B). Markers of inflammation (serum C-reactive protein [CRP], mRNA levels of *Saa1* [serum amyloid A1] and IL-6 in the liver) were also not significantly affected in response to the HFD (Fig. 4C to E). In addition, in both CD- and HFD-fed mice, concentrations of IL-6 in the serum were low and consistently below the detection limit (15.6 pg/mL) of the assay used, at all the time points studied. In addition, mRNA expression of proteins involved in duodenal iron absorption (divalent metal transporter-1, ferroportin and duodenal cytochrome b) was also not affected by HFD-feeding (data not shown).

3.5 Gene expression of erythroid regulators of hepcidin in erythroid precursor cells in the bone marrow was unaffected by the HFD

Expression of the erythroid regulators of hepcidin (*viz. Erfe*, *Gdf15* and *Twsg1*) in $Ter119^{+}$ cells isolated from the bone marrow (Fig. 5A–C), and serum erythropoietin levels (Fig. 5D), were not significantly affected by HFD-feeding. However, serum levels of GDF-15 were found to increase with increasing durations of feeding and were higher in HFD-fed mice,

especially from 16 weeks onwards (Fig. 5E). Hemoglobin levels in HFD- and CD-fed mice were similar at the various time points studied (data not shown).

3.6 The iron content in eWAT was higher in HFD-fed mice than in CD-fed mice

The type of diet fed had a significant effect on the iron content in the eWAT, with levels being higher in HFD-fed mice than in CD-fed animals (Fig. 6A). Although there was a significant interaction between diet and duration of feeding on mRNA levels of *Tfrc*, post-hoc analyses showed a significant difference between HFD- and CD-fed mice only at 8 weeks (Fig. 6B). Protein levels of ferritin tended to increase and that of ferroportin tended to decrease over time in the eWAT of both CD- and HFD-fed mice (Fig. 6C and D). Ferritin (L) protein levels in the eWAT from mice fed HFD were initially lower (significantly so at 12 weeks) than in those fed CD, and then became higher at some of the later time points (16 and 24 weeks) (Fig. 6C). Corresponding with this, ferroportin protein levels were also lower initially in the eWAT of HFD-fed mice than in CD-fed mice (significantly so at 12 weeks) and became higher in the HFD-fed mice than in CD-fed mice, by 24 weeks (Fig. 6D). The total iron content of the eWAT (iron content per gram adipose tissue multiplied by weight of eWAT) of HFD-fed mice increased with duration of feeding, with the increases being statistically significant when compared to CD-fed mice at 8 and 16 weeks. No significant differences were noted among CD-fed mice (Fig. 6E). A significant negative correlation was seen between the iron content in the liver and total iron content in the eWAT (Fig. 6F). *Hamp1* mRNA expression in eWAT was found to be very low and could not be reliably quantitated by qPCR (data not shown).

3.7 Linear regression analyses

Linear regression analysis showed that IR (as assessed by ITT) in HFD-fed mice was associated positively with liver triglyceride levels (P=0.001) and negatively with liver iron levels (P=0.068). In CD-fed mice, IR was negatively associated with eWAT iron content (P=0.007) (Supplementary Table 3). Hepatic *Hamp1* mRNA levels were found to be positively associated with serum ferritin levels in the CD-fed mice (P=0.001). On the other hand, in HFD-fed mice, it was associated positively with protein levels of TfR2 (P=0.042) and mRNA expression of BMP6 (P=0.009) in the liver (Supplementary Table 4). The liver triglyceride content in HFD-fed mice was positively associated with insulin resistance (AUC in ITT) (P=0.001) and serum GDF-15 levels (P=0.024) (Supplementary Table 5). Liver iron levels were positively associated with serum hepcidin in CD-fed mice (P=0.014), but not in HFD-fed mice (Supplementary Table 6).

A summary of the major findings of this study is provided in Supplementary table 7.

4 Discussion

C57Bl/6 mice fed a high-fat diet (HFD) develop many of the features of T2DM that are seen in humans [44–46]. However, prior to carrying out this study, it was not clear how HFD feeding affected systemic iron homeostasis. To the best of our knowledge, ours is the first study that has systematically documented the time-course of changes seen in iron-related parameters in a mouse model of IR.

The observed correlations of IR with hepatic steatosis and hepatic iron levels (Supplementary Table 3) are in agreement with previous literature in this area [47,48]. It has also been reported previously that mice fed HFD for 16 weeks had decreased liver iron stores [30,31]. Our results are in keeping with these reports. In the present study, since a significant increase in IR was seen from 12 weeks onwards and decreases in liver iron content from 16 weeks onwards, it appears that the onset of IR preceded that of dysregulated hepatic iron homeostasis in this model.

A decrease in intracellular iron levels, acting via the iron regulatory protein–iron response element (IRP-IRE) axis, has been shown to increase the stability of TfR1 mRNA [49]. Similarly, the IRP-IRE axis would also be expected to decrease the translation of ferroportin when intracellular iron decreases, thus decreasing ferroportin protein levels [50]. Consistent with this, we found a negative correlation between TfR1 mRNA levels and ferroportin protein levels in the liver. However, protein and mRNA levels of ferroportin were not significantly affected in HFD-fed mice at any of the time points studied (Fig. 3E and F). In addition, mRNA expression of duodenal proteins involved in iron absorption was also not affected. This suggests that iron absorption was unaffected in response to HFD-feeding. Hence, the mechanism that underlies the decrease in liver iron in mice fed the HFD remains unclear and requires further investigation.

Previous studies have shown that mice fed HFD for 16 weeks had decreased hepatic *Hamp1* expression [30,31]. *Hamp1* expression in the liver were also found to be decreased in *db/db* mice, another mouse model of obesity-induced IR [51]. In the present study, HFD-feeding had a significant effect on liver *Hamp1* mRNA and serum hepcidin levels with levels tending to be lower in HFD-fed mice at 16, 20 and 24 weeks (Fig. 2). The liver is the major site for iron storage in the body and *Hamp1* expression in the liver is known to be regulated by hepatic iron stores [21]. We show that the expected positive correlation between hepatic iron content and *Hamp1* expression was seen in CD-fed mice but not in those fed HFD (Supplementary Table 4). This suggests that, in the setting of HFD-feeding, this relationship seems to be lost and that there may be other factors that regulate hepcidin. Such factors include serum iron, inflammation, and the bone marrow erythroid regulators of hepcidin [14]. All of these were studied; none of them were significantly affected by HFD (Figs. 4 and 5). Linear regression analyses, however, showed that mRNA levels of BMP6 and protein levels of TfR2 were independently associated with hepatic *Hamp1* expression in HFD-fed mice (Supplementary Table 4).

GDF-15 is one of the putative erythroid regulators of hepcidin [52]. Recently, it has been shown that GDF-15 is produced in the liver and adipose tissue in response to high-fat feeding, where it has been suggested to play a role in governing energy homeostasis and signaling nutritional stress [53]. In the present study, although mRNA expression of GDF-15 in the bone marrow was not affected by HFD-feeding (Fig. 5B), serum levels of GDF-15 levels were found to be elevated, especially at 16, 20 and 24 weeks (Fig. 5E). It is possible that the liver and adipose tissue are the sources of the elevated GDF-15 in the blood, and that it may play a role in the regulation of hepcidin in this setting.

In the present study, we did not find evidence of hepatic inflammation (as indicated by lack of significant elevations in mRNA levels of liver *Saa1* and *IL-6* [Fig. 4D and E]) or systemic inflammation (as shown by absence of significant increases in serum CRP [Fig. 4C] or serum IL-6). These results are consistent with several reports that have shown that a high-fat diet alone is often insufficient to induce hepatic inflammation; these studies show that hepatic inflammation was induced only when mice were fed HFD along with sucrose [54], cholesterol [55–58] or both [59].

Obesity and insulin resistance have been shown to be associated with hypoadiponectinemia [60,61]. However, our results from the present study show that serum adiponectin levels were increased initially in HFD-fed mice, but started declining after 16 weeks of HFD-feeding to levels seen in CD-fed mice [Fig. 1H]). These findings are consistent with an earlier report which showed initial increases in adiponectin following HFD-feeding for up to 10 weeks, which was positively correlated with diet-induced expansion of the adipose tissue [62]. In the same study, HFD-feeding for 18 weeks resulted in serum adiponectin levels similar to those in CD-fed mice, and this was associated with a reduction in mRNA expression of adiponectin in the eWAT of these mice.

Iron is essential for adipocyte differentiation and mitochondrial biogenesis. Expansion of adipose tissue depots in response to HFD feeding is therefore associated with increased iron demands [63,64]. An earlier report has shown that HFD feeding in mice altered tissue iron distribution, resulting in a decrease in liver iron and a concomitant increase in iron levels in the adipose tissue [32]. Our results are consistent with this report. In addition, protein levels of ferroportin in the eWAT were significantly lower in HFD-fed mice than in CD-fed mice, at some of the time points studied (Fig. 6D). This suggests that a decrease in iron efflux may underlie the increase seen in the iron content of the adipose tissue. The total iron content of the eWAT was inversely correlated with liver iron content (Fig. 6F). These observations are in agreement with recent reports that showed that hepatic iron stores were inversely proportional to body adiposity [31] and were restored to normal by feeding HFD-fed obese mice with a low-fat diet [65]. It has been shown, both in humans [66] and in mice [32,67], that dysregulation of adipose tissue iron homeostasis is associated with IR. In addition, adipocyte iron has been shown to regulate the expression of adipokines, such as adiponectin [68] and leptin [69], which play critical roles in energy homeostasis. It is therefore possible the HFD-induced increases in iron in adipose tissue may play a role in exacerbation of IR in this setting.

Differences in iron metabolism are known to exist in males and females, both in mice and humans [70,71]. Gender-related differences have also been reported in the response of mice to high-fat feeding [72]. In view of this, we confined our studies to male mice only, in order to avoid possible confounding due to gender. The fact that female mice were not studied is a limitation of the present study.

5 Conclusions

The results of this time-course study show that the onset of IR in HFD-fed mice preceded reductions in hepatic iron content and other alterations in iron-related parameters. This was

associated with a decrease in hepcidin levels. HFD did not affect serum iron levels, markers of inflammation or expression of the erythroid regulators of hepcidin in the bone marrow. Decreases in liver iron levels in response to HFD-feeding were associated with a coincident increase in the iron content in the adipose tissue. Whether such increases in adipose tissue iron play a role in development of IR is, however, unclear. Elucidation of this would require further investigation.

Supplementary Material

Refer to Web version on PubMed Central for supplementary material.

Funding

☆ This work was funded by an Early Career Fellowship awarded to Joe Varghese by the Wellcome Trust-DBT India Alliance (Ref no. 500190/Z/11/Z).

References

[1]. Johnson AMF, Olefsky JM. The origins and drivers of insulin resistance. Cell. 2013; 152:673–84. DOI: 10.1016/j.cell.2013.01.041 [PubMed: 23415219]

[2]. Ford ES, Cogswell ME. Diabetes and serum ferritin concentration among U.S. adults. Diabetes Care. 1999; 22:1978–83. [PubMed: 10587829]

[3]. Haap M, Fritsche A, Mensing HJ, Häring H-U, Stumvoll M. Association of high serum ferritin concentration with glucose intolerance and insulin resistance in healthy people. Ann Intern Med. 2003; 139:869–71.

[4]. Jiang R, Manson JE, Meigs JB, Ma J, Rifai N, Hu FB. Body iron stores in relation to risk of type 2 diabetes in apparently healthy women. JAMA J Am Med Assoc. 2004; 291:711–7. DOI: 10.1001/jama.291.6.711

[5]. Acton RT, Barton JC, Passmore LV, Adams PC, Speechley MR, Dawkins FW, et al. Relationships of serum ferritin, transferrin saturation, and HFE mutations and self-reported diabetes in the hemochromatosis and Iron overload screening (HEIRS) study. Diabetes Care. 2006; 29:2084–9. DOI: 10.2337/dc05-1592 [PubMed: 16936157]

[6]. Forouhi NG, Harding AH, Allison M, Sandhu MS, Welch A, Luben R, et al. Elevated serum ferritin levels predict new-onset type 2 diabetes: results from the EPIC-Norfolk prospective study. Diabetologia. 2007; 50:949–56. DOI: 10.1007/s00125-007-0604-5 [PubMed: 17333112]

[7]. Baynes R, Bezwoda W, Bothwell T, Khan Q, Mansoor N. The non-immune inflammatory response: serial changes in plasma iron, iron-binding capacity, lactoferrin, ferritin and C-reactive protein. Scand J Clin Lab Invest. 1986; 46:695–704. [PubMed: 3787168]

[8]. Brailsford S, Lunec J, Winyard P, Blake DR. A possible role for ferritin during inflammation. Free Radic Res Commun. 1985; 1:101–9. [PubMed: 2853105]

[9]. Dandona P, Aljada A, Bandyopadhyay A. Inflammation: the link between insulin resistance, obesity and diabetes. Trends Immunol. 2004; 25:4–7. [PubMed: 14698276]

[10]. Podmore C, Meidtner K, Schulze MB, Scott RA, Ramond A, Butterworth AS, et al. Association of Multiple Biomarkers of Iron metabolism and type 2 diabetes: the EPIC-InterAct study. Diabetes Care. 2016; 39:572–81. DOI: 10.2337/dc15-0257 [PubMed: 26861925]

[11]. Jehn M, Clark JM, Guallar E. Serum ferritin and risk of the metabolic syndrome in U.S. adults. Diabetes Care. 2004; 27:2422–8. [PubMed: 15451911]

[12]. Fernández-Real JM, Peñarroja G, Castro A, García-Bragado F, Hernández-Aguado I, Ricart W. Blood letting in high-ferritin type 2 diabetes: effects on insulin sensitivity and beta-cell function. Diabetes. 2002; 51:1000–4. [PubMed: 11916918]

[13]. Facchini FS. Effect of phlebotomy on plasma glucose and insulin concentrations. Diabetes Care. 1998; 21:2190.

[14]. Ganz T. Hepcidin and iron regulation, 10 years later. Blood. 2011; 117:4425–33. DOI: 10.1182/blood-2011-01-258467 [PubMed: 21346250]

[15]. Andrews NC. Forging a field: the golden age of iron biology. Blood. 2008; 112:219–30. DOI: 10.1182/blood-2007-12-077388 [PubMed: 18606887]

[16]. Babitt JL, Huang FW, Xia Y, Sidis Y, Andrews NC, Lin HY. Modulation of bone morphogenetic protein signaling in vivo regulates systemic iron balance. J Clin Invest. 2007; 117:1933–9. DOI: 10.1172/JCI31342 [PubMed: 17607365]

[17]. Canali S, Zumbrennen-Bullough KB, Core AB, Wang C-Y, Nairz M, Bouley R, et al. Endothelial cells produce bone morphogenetic protein 6 required for iron homeostasis in mice. Blood. 2017; 129:405–14. DOI: 10.1182/blood-2016-06-721571 [PubMed: 27864295]

[18]. Andriopoulos B Jr, Corradini E, Xia Y, Faasse SA, Chen S, Grgurevic L, et al. BMP6 is a key endogenous regulator of hepcidin expression and iron metabolism. Nat Genet. 2009; 41:482–7. DOI: 10.1038/ng.335 [PubMed: 19252486]

[19]. Finberg KE, Whittlesey RL, Fleming MD, Andrews NC. Down-regulation of bmp/Smad signaling by Tmprss6 is required for maintenance of systemic iron homeostasis. Blood. 2010; 115:3817–26. DOI: 10.1182/blood-2009-05-224808 [PubMed: 20200349]

[20]. Folgueras AR, de Lara FM, Pendás AM, Garabaya C, Rodríguez F, Astudillo A, et al. Membrane-bound serine protease matriptase-2 (Tmprss6) is an essential regulator of iron homeostasis. Blood. 2008; 112:2539–45. DOI: 10.1182/blood-2008-04-149773 [PubMed: 18523150]

[21]. Corradini E, Meynard D, Wu Q, Chen S, Ventura P, Pietrangelo A, et al. Serum and liver iron differently regulate the bone morphogenetic protein 6 (BMP6)-SMAD signaling pathway in mice. Hepatol Baltim Md. 2011; 54:273–84. DOI: 10.1002/hep.24359

[22]. Meynard D, Vaja V, Sun CC, Corradini E, Chen S, López-Otín C, et al. Regulation of TMPRSS6 by BMP6 and iron in human cells and mice. Blood. 2011; 118:747–56. DOI: 10.1182/blood-2011-04-348698 [PubMed: 21622652]

[23]. Zhang A-S, Anderson SA, Wang J, Yang F, DeMaster K, Ahmed R, et al. Suppression of hepatic hepcidin expression in response to acute iron deprivation is associated with an increase of matriptase-2 protein. Blood. 2011; 117:1687–99. DOI: 10.1182/blood-2010-06-287292 [PubMed: 21115976]

[24]. Pasricha S-R, McHugh K, Drakesmith H. Regulation of Hepcidin by erythropoiesis: the story so far. Annu Rev Nutr. 2016; 36:417–34. DOI: 10.1146/annurev-nutr-071715-050731 [PubMed: 27146013]

[25]. Bersch N, Groopman JE, Golde DW. Natural and biosynthetic insulin stimulates the growth of human erythroid progenitors in vitro. J Clin Endocrinol Metab. 1982; 55:1209–11. DOI: 10.1210/jcem-55-6-1209 [PubMed: 6752170]

[26]. Kurtz A, Jelkmann W, Bauer C. Insulin stimulates erythroid colony formation independently of erythropoietin. Br J Haematol. 1983; 53:311–6. [PubMed: 6336950]

[27]. Haffner SM, Stern MP, Hazuda HP, Pugh JA, Patterson JK. Hyperinsulinemia in a population at high risk for non-insulin-dependent diabetes mellitus. N Engl J Med. 1986; 315:220–4. DOI: 10.1056/NEJM198607243150403 [PubMed: 3523246]

[28]. Nemeth E, Rivera S, Gabayan V, Keller C, Taudorf S, Pedersen BK, et al. IL-6 mediates hypoferremia of inflammation by inducing the synthesis of the iron regulatory hormone hepcidin. J Clin Invest. 2004; 113:1271–6. DOI: 10.1172/JCI20945 [PubMed: 15124018]

[29]. Wellen KE, Hotamisligil GS. Obesity-induced inflammatory changes in adipose tissue. J Clin Invest. 2003; 112:1785–8. DOI: 10.1172/JCI20514 [PubMed: 14679172]

[30]. Chung J, Kim MS, Han SN. Diet-induced obesity leads to decreased hepatic iron storage in mice. Nutr Res N Y N. 2011; 31:915–21. DOI: 10.1016/j.nutres.2011.09.014

[31]. Park CY, Chung J, Koo K-O, Kim MS, Han SN. Hepatic iron storage is related to body adiposity and hepatic inflammation. Nutr Metab. 2017; 14:14.doi: 10.1186/s12986-017-0169-3

[32]. Orr JS, Kennedy A, Anderson-Baucum EK, Webb CD, Fordahl SC, Erikson KM, et al. Obesity alters adipose tissue macrophage iron content and tissue iron distribution. Diabetes. 2014; 63:421–32. DOI: 10.2337/db13-0213 [PubMed: 24130337]

[33]. Winzell MS, Ahrén B. The high-fat diet-fed mouse: a model for studying mechanisms and treatment of impaired glucose tolerance and type 2 diabetes. Diabetes. 2004; 53(Suppl. 3):S215–9. [PubMed: 15561913]

[34]. [accessed October 20, 2017] OpenSource Diets - Stock Diets - DIO Series Diets - Research Diets, Inc n.d. http://www.researchdiets.com/opensource-diets/stock-diets/dio-series-diets

[35]. [accessed November 3, 2017] Diets. SAFE DIETS n.d. http://www.safe-diets.com/en/products/diets/

[36]. Casteilla L, Pénicaud L, Cousin B, Calise D. Choosing an adipose tissue depot for sampling: factors in selection and depot specificity. Methods Mol Biol Clifton NJ. 2008; 456:23–38. DOI: 10.1007/978-1-59745-245-8_2

[37]. Kilkenny C, Browne WJ, Cuthill IC, Emerson M, Altman DG. Improving bioscience research reporting: the ARRIVE guidelines for reporting animal research. PLoS Biol. 2010; 8:e1000412.doi: 10.1371/journal.pbio.1000412 [PubMed: 20613859]

[38]. Andrikopoulos S, Blair AR, Deluca N, Fam BC, Proietto J. Evaluating the glucose tolerance test in mice. Am J Physiol Endocrinol Metab. 2008; 295:E1323–32. DOI: 10.1152/ajpendo.90617.2008 [PubMed: 18812462]

[39]. Ayala JE, Samuel VT, Morton GJ, Obici S, Croniger CM, Shulman GI, et al. Standard operating procedures for describing and performing metabolic tests of glucose homeostasis in mice. Dis Model Mech. 2010; 3:525–34. DOI: 10.1242/dmm.006239 [PubMed: 20713647]

[40]. Koulnis M, Pop R, Porpiglia E, Shearstone JR, Hidalgo D, Socolovsky M. Identification and analysis of mouse erythroid progenitors using the CD71/TER119 flow-cytometric assay. J Vis Exp JoVE. 2011; doi: 10.3791/2809

[41]. Varghese J, James JV, Sagi S, Chakraborty S, Sukumaran A, Ramakrishna B, et al. Decreased hepatic iron in response to alcohol may contribute to alcohol-induced suppression of hepcidin. Br J Nutr. 2016; 115:1978–86. DOI: 10.1017/S0007114516001197 [PubMed: 27080262]

[42]. Pitman JL, Bonnet DJ, Curtiss LK, Gekakis N. Reduced cholesterol and triglycerides in mice with a mutation in Mia2, a liver protein that localizes to ER exit sites. J Lipid Res. 2011; 52:1775–86. DOI: 10.1194/jlr.M017277 [PubMed: 21807889]

[43]. Brunt EM, Janney CG, Di Bisceglie AM, Neuschwander-Tetri BA, Bacon BR. Nonalcoholic steatohepatitis: a proposal for grading and staging the histological lesions. Am J Gastroenterol. 1999; 94:2467–74. DOI: 10.1111/j.1572-0241.1999.01377.x [PubMed: 10484010]

[44]. Collins S, Martin TL, Surwit RS, Robidoux J. Genetic vulnerability to diet-induced obesity in the C57BL/6J mouse: physiological and molecular characteristics. Physiol Behav. 2004; 81:243–8. DOI: 10.1016/j.physbeh.2004.02.006 [PubMed: 15159170]

[45]. Petro AE, Cotter J, Cooper DA, Peters JC, Surwit SJ, Surwit RS. Fat carbohydrate, and calories in the development of diabetes and obesity in the C57BL/6J mouse. Metabolism. 2004; 53:454–7. [PubMed: 15045691]

[46]. Rossmeisl M, Rim JS, Koza RA, Kozak LP. Variation in type 2 diabetes–related traits in mouse strains susceptible to diet-induced obesity. Diabetes. 2003; 52:1958–66. [PubMed: 12882911]

[47]. Perry RJ, Samuel VT, Petersen KF, Shulman GI. The role of hepatic lipids in hepatic insulin resistance and type 2 diabetes. Nature. 2014; 510:84–91. DOI: 10.1038/nature13478 [PubMed: 24899308]

[48]. Britton L, Bridle K, Reiling J, Santrampurwala N, Wockner L, Ching H, et al. Hepatic iron concentration correlates with insulin sensitivity in nonalcoholic fatty liver disease. Hepatol Commun. 2018; 2:644–53. DOI: 10.1002/hep4.1190 [PubMed: 29881816]

[49]. Hentze MW, Kühn LC. Molecular control of vertebrate iron metabolism: mRNA-based regulatory circuits operated by iron, nitric oxide, and oxidative stress. Proc Natl Acad Sci U S A. 1996; 93:8175–82. [PubMed: 8710843]

[50]. Lymboussaki A, Pignatti E, Montosi G, Garuti C, Haile DJ, Pietrangelo A. The role of the iron responsive element in the control of ferroportin1/IREG1/MTP1 gene expression. J Hepatol. 2003; 39:710–5. DOI: 10.1016/s0168-8278(03)00408-2 [PubMed: 14568251]

[51]. Altamura S, Kopf S, Schmidt J, Müdder K, da Silva AR, Nawroth P, et al. Uncoupled iron homeostasis in type 2 diabetes mellitus. J Mol Med Berl Ger. 2017; doi: 10.1007/s00109-017-1596-3

[52]. Tanno T, Bhanu NV, Oneal PA, Goh S-H, Staker P, Lee YT, et al. High levels of GDF15 in thalassemia suppress expression of the iron regulatory protein hepcidin. Nat Med. 2007; 13:1096–101. DOI: 10.1038/nm1629 [PubMed: 17721544]

[53]. Patel S, Alvarez-Guaita A, Melvin A, Rimmington D, Dattilo A, Miedzybrodzka EL, et al. GDF15 Provides an Endocrine Signal of Nutritional Stress in Mice and Humans. Cell Metab. 2019; 29:707–18 e8. DOI: 10.1016/j.cmet.2018.12.016 [PubMed: 30639358]

[54]. Ishimoto T, Lanaspa MA, Rivard CJ, Roncal-Jimenez CA, Orlicky DJ, Cicerchi C, et al. High-fat and high-sucrose (western) diet induces steatohepatitis that is dependent on fructokinase. Hepatol Baltim Md. 2013; 58:1632–43. DOI: 10.1002/hep.26594

[55]. Li S, Zeng X-Y, Zhou X, Wang H, Jo E, Robinson SR, et al. Dietary cholesterol induces hepatic inflammation and blunts mitochondrial function in the liver of high-fat-fed mice. J Nutr Biochem. 2016; 27:96–103. DOI: 10.1016/j.jnutbio.2015.08.021 [PubMed: 26391864]

[56]. Wouters K, van Gorp PJ, Bieghs V, Gijbels MJ, Duimel H, Lütjohann D, et al. Dietary cholesterol, rather than liver steatosis, leads to hepatic inflammation in hyperlipidemic mouse models of nonalcoholic steatohepatitis. Hepatol Baltim Md. 2008; 48:474–86. DOI: 10.1002/hep.22363

[57]. Savard C, Tartaglione EV, Kuver R, Haigh WG, Farrell GC, Subramanian S, et al. Synergistic interaction of dietary cholesterol and dietary fat in inducing experimental steatohepatitis. Hepatol Baltim Md. 2013; 57:81–92. DOI: 10.1002/hep.25789

[58]. Clapper JR, Hendricks MD, Gu G, Wittmer C, Dolman CS, Herich J, et al. Diet-induced mouse model of fatty liver disease and nonalcoholic steatohepatitis reflecting clinical disease progression and methods of assessment. Am J Physiol Gastrointest Liver Physiol. 2013; 305:G483–95. DOI: 10.1152/ajpgi.00079.2013 [PubMed: 23886860]

[59]. Dorn C, Engelmann JC, Saugspier M, Koch A, Hartmann A, Müller M, et al. Increased expression of c-Jun in nonalcoholic fatty liver disease. Lab Investig J Tech Methods Pathol. 2014; 94:394–408. DOI: 10.1038/labinvest.2014.3

[60]. Arita Y, Kihara S, Ouchi N, Takahashi M, Maeda K, Miyagawa J, et al. Paradoxical decrease of an adipose-specific protein, adiponectin, in obesity. Biochem Biophys Res Commun. 1999; 257:79–83. DOI: 10.1006/bbrc.1999.0255 [PubMed: 10092513]

[61]. Hu E, Liang P, Spiegelman BM. AdipoQ is a novel adipose-specific gene dysregulated in obesity. J Biol Chem. 1996; 271:10697–703. DOI: 10.1074/jbc.271.18.10697 [PubMed: 8631877]

[62]. Bullen JW, Bluher S, Kelesidis T, Mantzoros CS. Regulation of adiponectin and its receptors in response to development of diet-induced obesity in mice. Am J Physiol Endocrinol Metab. 2007; 292:E1079–86. DOI: 10.1152/ajpendo.00245.2006 [PubMed: 17164441]

[63]. Moreno-Navarrete JM, Ortega F, Moreno M, Ricart W, Fernández-Real JM. Fine-tuned iron availability is essential to achieve optimal adipocyte differentiation and mitochondrial biogenesis. Diabetologia. 2014; 57:1957–67. DOI: 10.1007/s00125-014-3298-5 [PubMed: 24973963]

[64]. Festa M, Ricciardelli G, Mele G, Pietropaolo C, Ruffo A, Colonna A. Overexpression of H ferritin and up-regulation of iron regulatory protein genes during differentiation of 3T3-L1 pre-adipocytes. J Biol Chem. 2000; 275:36708–12. DOI: 10.1074/jbc.M004988200 [PubMed: 10978328]

[65]. Chung H, Wu D, Smith D, Meydani SN, Han SN. Lower hepatic iron storage associated with obesity in mice can be restored by decreasing body fat mass through feeding a low-fat diet. Nutr Res N Y N. 2016; 36:955–63. DOI: 10.1016/j.nutres.2016.06.003

[66]. Moreno-Navarrete JM, Novelle MG, Catalán V, Ortega F, Moreno M, Gomez-Ambrosi J, et al. Insulin resistance modulates iron-related proteins in adipose tissue. Diabetes Care. 2014; 37:1092–100. DOI: 10.2337/dc13-1602 [PubMed: 24496804]

[67]. Dongiovanni P, Ruscica M, Rametta R, Recalcati S, Steffani L, Gatti S, et al. Dietary iron overload induces visceral adipose tissue insulin resistance. Am J Pathol. 2013; 182:2254–63. DOI: 10.1016/j.ajpath.2013.02.019 [PubMed: 23578384]

[68]. Gabrielsen JS, Gao Y, Simcox JA, Huang J, Thorup D, Jones D, et al. Adipocyte iron regulates adiponectin and insulin sensitivity. J Clin Invest. 2012; 122:3529–40. DOI: 10.1172/JCI44421 [PubMed: 22996660]

[69]. Gao Y, Li Z, Gabrielsen JS, Simcox JA, Lee S, Jones D, et al. Adipocyte iron regulates leptin and food intake. J Clin Invest. 2015; 125:3681–91. DOI: 10.1172/JCI81860 [PubMed: 26301810]

[70]. Courselaud B, Troadec M-B, Fruchon S, Ilyin G, Borot N, Leroyer P, et al. Strain and gender modulate hepatic hepcidin 1 and 2 mRNA expression in mice. Blood Cells Mol Dis. 2004; 32:283–9. DOI: 10.1016/j.bcmd.2003.11.003 [PubMed: 15003819]

[71]. Harrison-Findik DD. Gender-related variations in iron metabolism and liver diseases. World J Hepatol. 2010; 2:302–10. DOI: 10.4254/wjh.v2.i8.302 [PubMed: 21161013]

[72]. Ganz M, Csak T, Szabo G. High fat diet feeding results in gender specific steatohepatitis and inflammasome activation. World J Gastroenterol WJG. 2014; 20:8525–34. DOI: 10.3748/wjg.v20.i26.8525 [PubMed: 25024607]

Europe PMC Funders Author Manuscripts

Europe PMC Funders Author Manuscripts

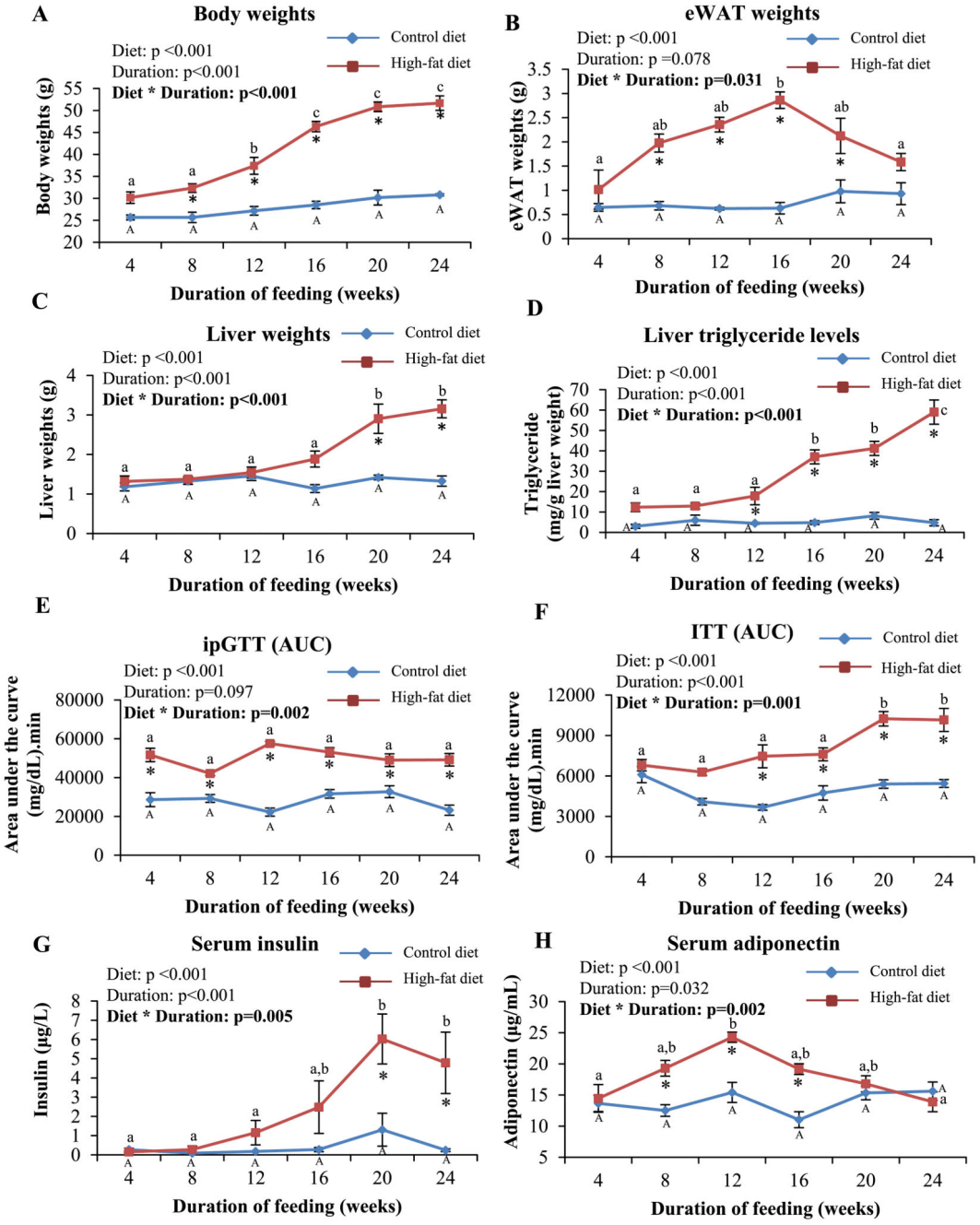

Fig. 1. High-fat feeding induced progressive weight gains, hepatosteatosis, glucose intolerance, insulin resistance and hyperinsulinemia in mice.

A-C: Body (A), eWAT (B) and liver (C) weights in CD and HFD-fed mice at the end of each time point of feeding are shown. *D:* Triglyceride levels in the liver. *E and F*: Intraperitoneal glucose tolerance (E) and insulin tolerance (F) tests. Data are represented as area-under-curve [AUC] calculated by the linear trapezoidal method. *G and H*: Serum levels of insulin (non-fasting) (G) and adiponectin (H) estimated by ELISA. Data are shown as means ± SE; n=6 at each time point (for both CD- and HFD-fed mice). Data were analyzed by two-way ANOVA with post-hoc Bonferroni test. * indicates P<0.05 when HFD-fed mice are

compared to the respective CD-fed group. Different alphabets indicate groups that are significantly different from one another; upper-case letters are used specifically only for mice fed CD for different durations to denote significant differences between these, while lower-case letters are used specifically only for HFD-fed mice for the same purpose.

Europe PMC Funders Author Manuscripts

Europe PMC Funders Author Manuscripts

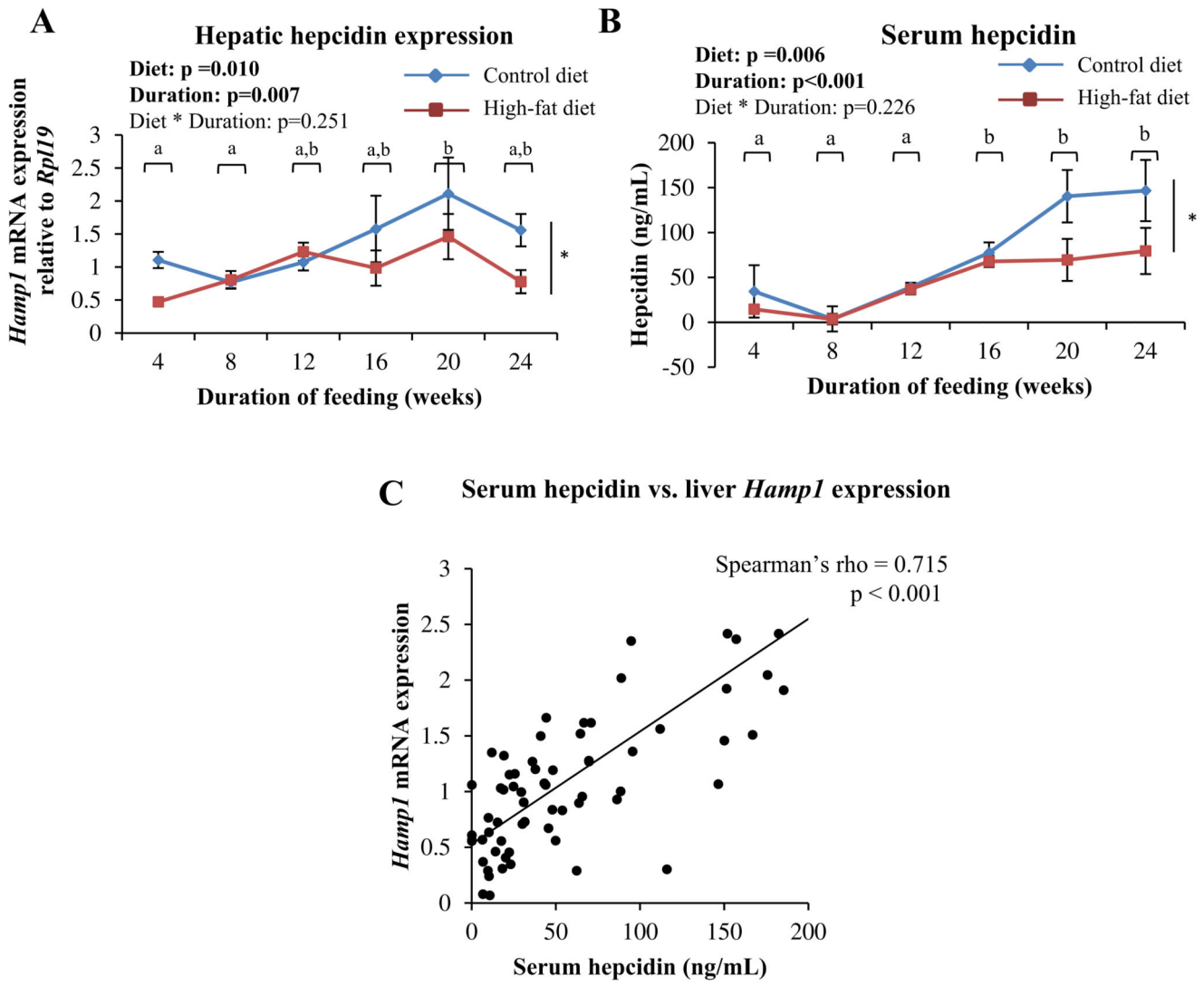

Fig. 2. HFD-feeding resulted in decreased hepatic Hamp1 expression and serum hepcidin levels.

A: Hepatic *Hamp1* mRNA expression, determined by qPCR. *B:* Serum hepcidin levels, estimated by ELISA. Data are shown as means ± SE; n=6 (for both CD- and HFD-fed mice) at each time point. In A and B, data were analyzed by two-way ANOVA with post-hoc Bonferroni test. Since no significant interaction between diet and duration of feeding was detected, the main effects (diet and duration of feeding) were considered. * indicates a statistically significant effect of the type of diet. Time points labeled with different alphabets are significantly different from one another. C: Scatter plot showing correlation between serum hepcidin and hepatic *Hamp1* expression (Spearman's correlation analysis).

Europe PMC Funders Author Manuscripts

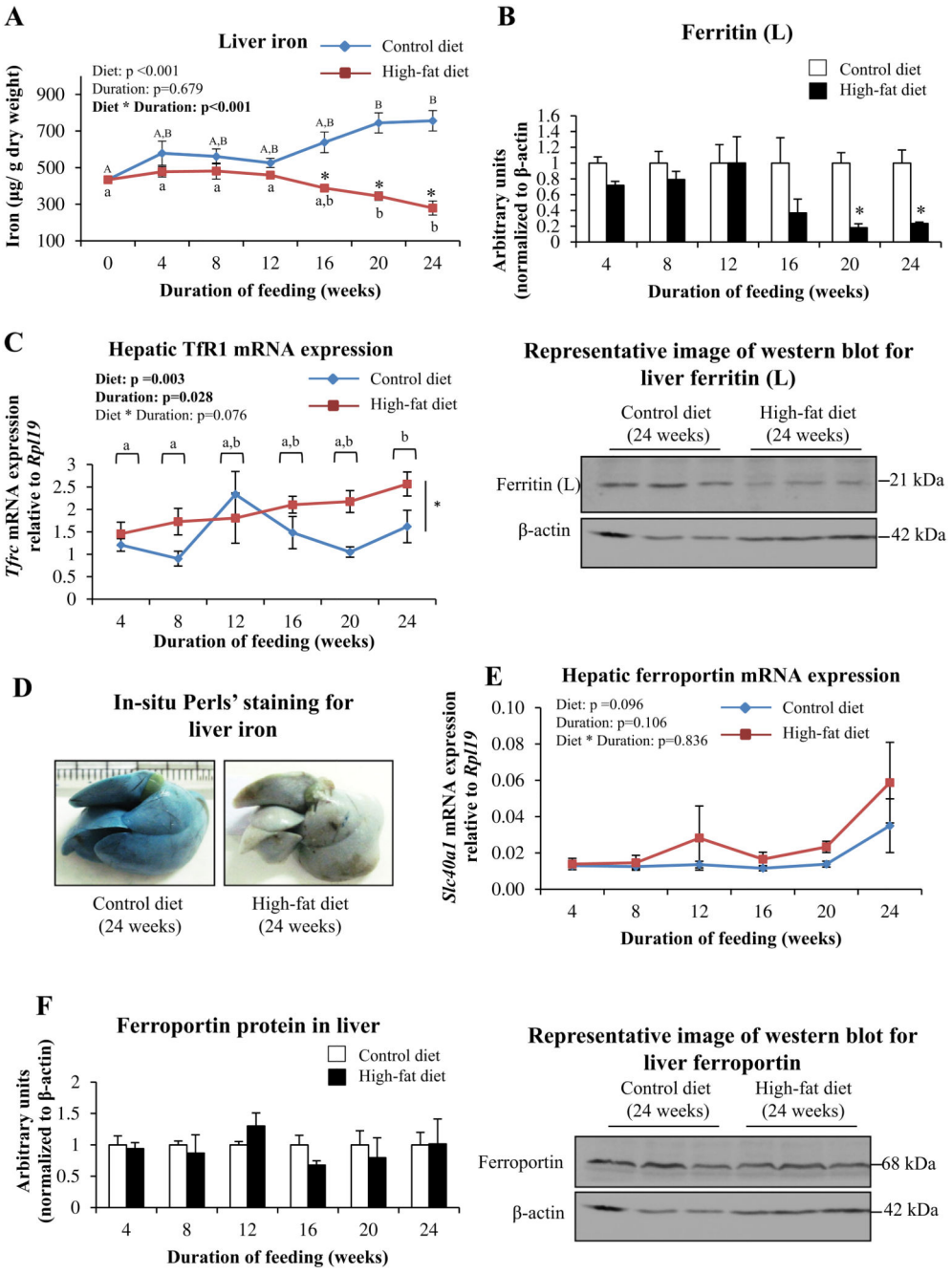

Fig. 3. HFD-feeding decreased hepatic iron content.

A: Liver iron levels, as estimated by bathophenanthroline-dye binding method. *B:* Protein levels of ferritin (L), as determined by western blotting. Representative blot from mice fed CD or HFD for 24 weeks is shown. *C:* Hepatic *Tfrc* (TfR1) mRNA expression, as determined by qPCR. *D:* Representative images of *in situ* Perls' perfusion staining for iron in livers of mice fed CD or HFD for 24 weeks. *E:* Hepatic *Slc40a1* (ferroportin) expression, as determined by qPCR. *F:* Protein levels of ferroportin, as determined by western blotting. Representative blots from mice fed CD or HFD for 24 weeks are shown. Data are shown as

mean±S.E.; n=6 (for both CD- and HFD-fed mice) at each time point. For A, C and E, statistical analysis was done by two-way ANOVA and post-hoc Bonferroni test (wherever applicable). In A, * indicates P<0.05 when HFD-fed mice are compared to the respective CD-fed group. Different alphabets indicate groups that are significantly different from one another; upper-case letters are used specifically to denote significant differences between mice fed CD for different durations, while lower-case letters are used specifically for HFD-fed mice. For B and F, data for HFD-fed mice at each time point studied was normalized to that from corresponding CD-fed mice; one-way ANOVA and post-hoc Bonferroni test were used for these analyses. * indicates P<0.05 when compared to the respective CD-fed group.

Europe PMC Funders Author Manuscripts

Europe PMC Funders Author Manuscripts

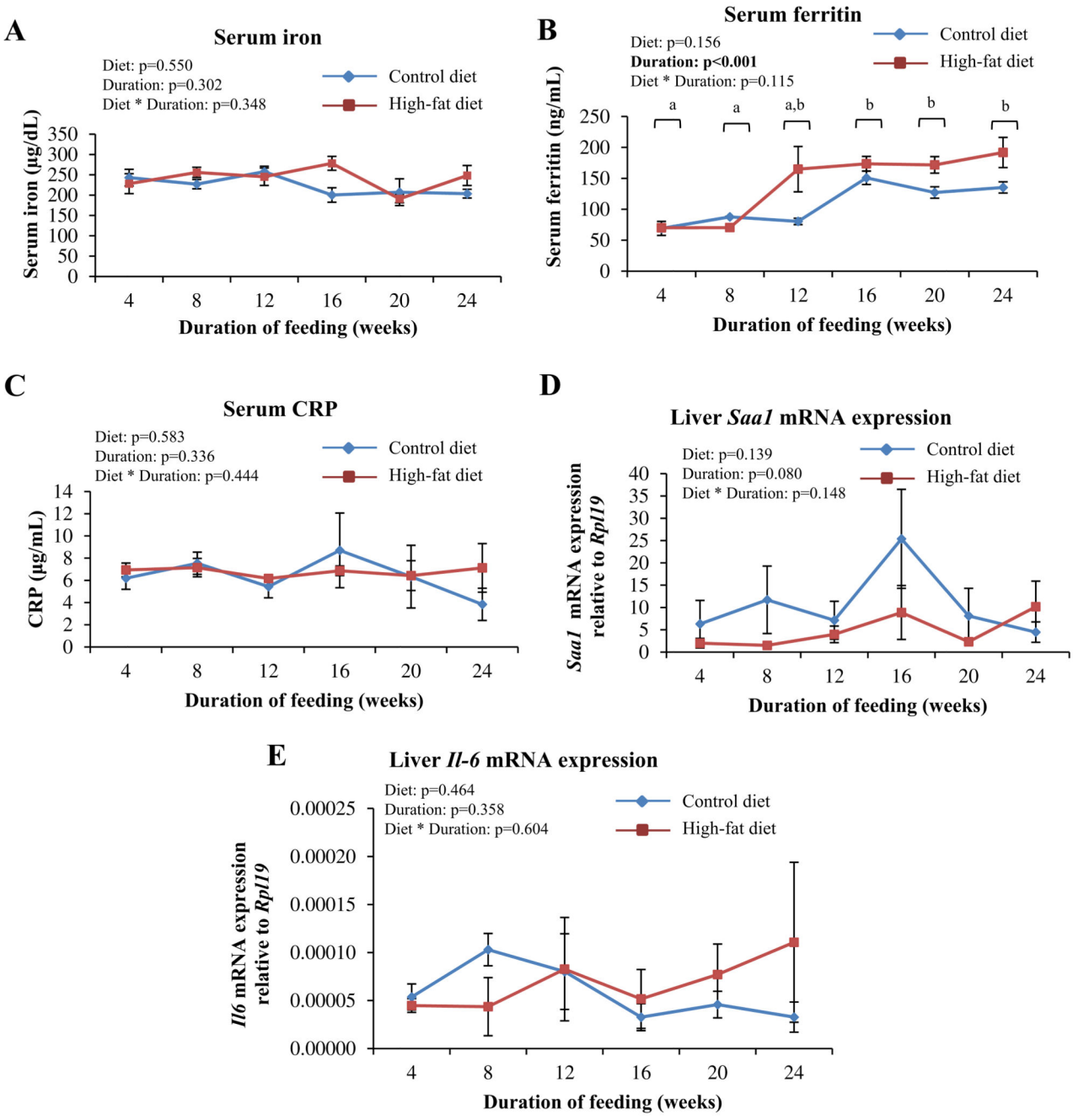

Fig. 4. HFD-feeding did not affect serum iron levels and markers of inflammation.

A: Serum levels of iron, as estimated by bathophenanthroline-dye binding method. *B* and *C:* Serum levels of ferritin (B) and CRP (C), as estimated by ELISA. *D* and *E:* Hepatic *Saa1* (D) and *Il6* (E) mRNA expression, as determined by qPCR. Data are shown as mean±S.E.; n=6 for A and D, n=3 for B, C and E at each time point (for both CD- and HFD-fed mice). Statistical analysis was done by two-way ANOVA and post-hoc Bonferroni test. In 4B, where a significant effect of duration of feeding was detected, time points labeled with different alphabets are significantly different from one another.

Europe PMC Funders Author Manuscripts

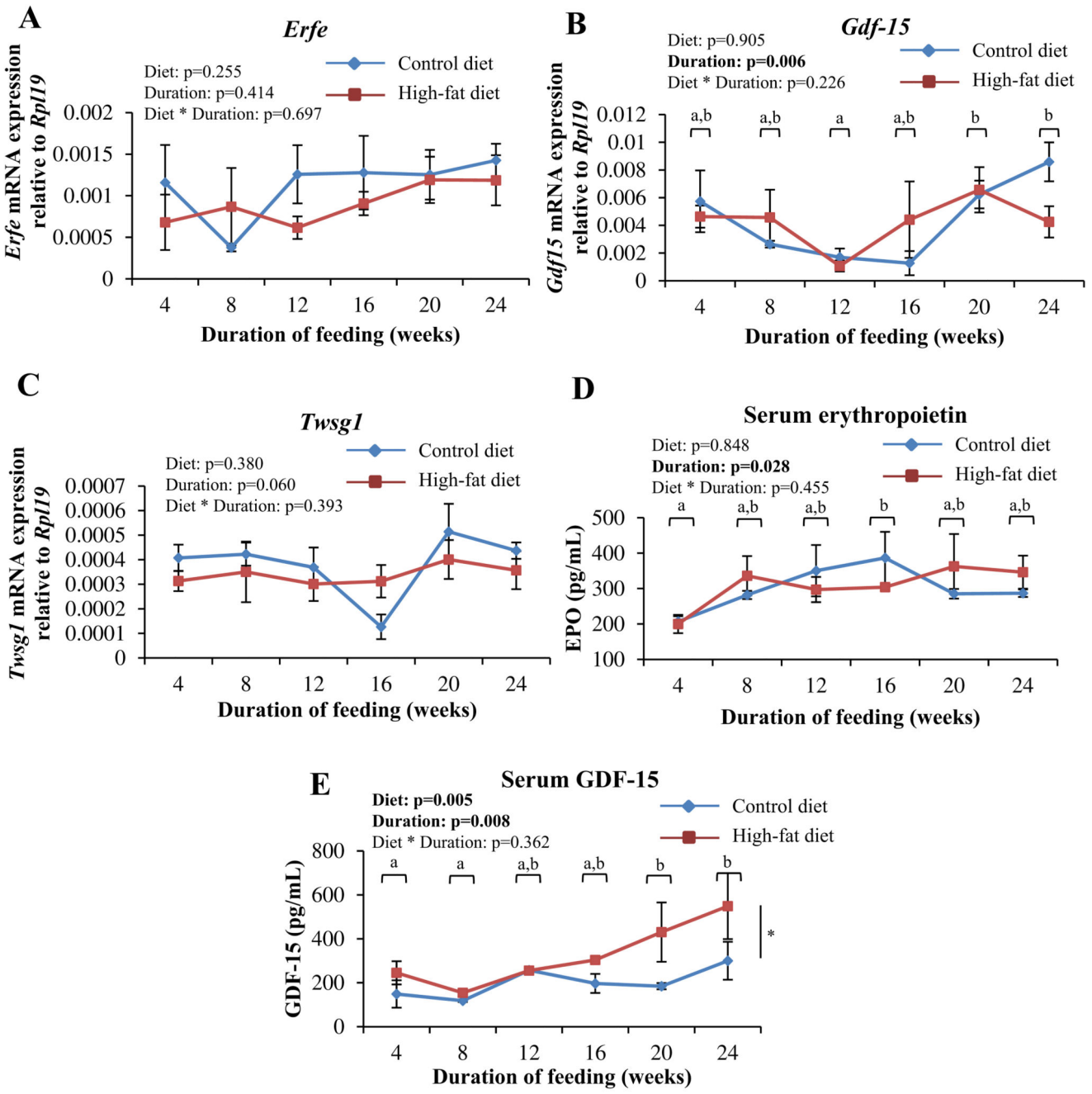

Fig. 5. HFD-feeding increased serum levels of GDF-15 but did not affect gene expression of the erythroid regulators of hepcidin in the bone marrow.

A-C: Gene expression of *Erfe* (A), *Gdf15* (B) and *Twsg1* (C) in TER119+ cells isolated from the bone marrow, as determined by qPCR. *D* and *E:* Serum levels of erythropoietin (D) and GDF-15 (E), as estimated by ELISA. Data are shown as mean±S.E.. n=6 for A, B, and C, n=3 for D and E (for both CD- and HFD-fed mice) at each time point.. Statistical analysis was done by two-way ANOVA and post-hoc Bonferroni test. In B, D and E, time points labeled with different alphabets are significantly different from one another. In E, * indicates a statistically significant effect of the type of diet.

Europe PMC Funders Author Manuscripts

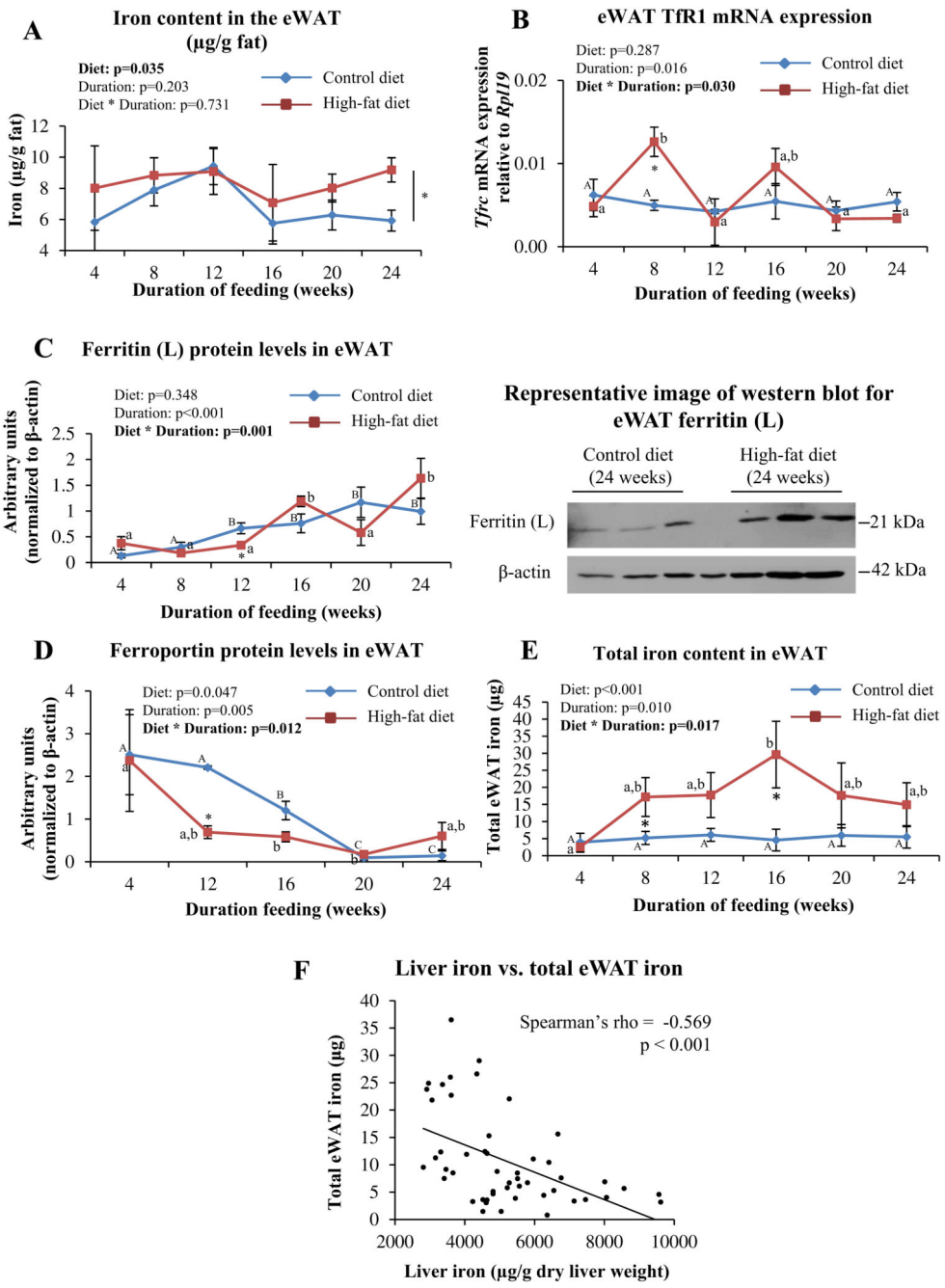

Fig. 6. HFD-feeding affected iron homeostasis in eWAT.

A: Iron content in eWAT (µg/g fat), estimated by AAS. *B:* eWAT *Tfrc* (TfR1) mRNA expression, as determined by qPCR. *C and D:* Protein levels of ferritin (C) and ferroportin (D), as determined by western blotting, in eWAT. Representative blots from mice fed CD or HFD for 24 weeks are shown. *E:* Total iron content in eWAT (iron content per gram eWAT multiplied by eWAT weight). *F:* Scatter plot showing correlation between iron levels in the liver and total iron content in eWAT.Data are shown as mean±S.E.; n=6 for A and E; n=3 for B, C and D (for both CD- and HFD-fed mice) at each time point. Statistical analysis was

done by two-way ANOVA and post-hoc Bonferroni test. In panel A, * indicates a significant effect of the type of diet. In panels B, C, D and E, a significant interaction between diet and duration of feeding was noted. In these panels, * indicates $P<0.05$ when HFD-fed mice are compared to the respective CD-fed group. Different alphabets indicate groups that are significantly different from one another; upper-case letters are used specifically to denote significant differences between mice fed CD for different durations, while lower-case letters are used specifically for HFD-fed mice. In F, Spearman's correlation analysis was done.

Europe PMC Funders Author Manuscripts